

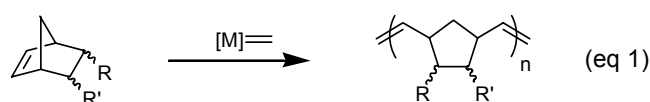
**Chapter 5:**  
**Ring-Opening Metathesis Polymerization with an Ultra-**  
**fast-initiating Ruthenium Catalyst**

## Abstract

Ring-opening metathesis polymerization (ROMP) is one of the most widely used polymerizations. With the development of well-defined catalysts, such as  $(t\text{-BuO})_2(\text{ArN})\text{-Mo=CH}(t\text{-Bu})$  (**1**),  $\text{Cl}_2(\text{PCy}_3)_2\text{Ru=CHPh}$  (**2**), and  $\text{Cl}_2(\text{PCy}_3)(\text{IMesH}_2)\text{Ru=CHPh}$  (**3**), more controlled polymer structures have been obtained by either living polymerization or chain transfer induced polymerization. However, these catalysts suffer from a number of limitations. This chapter describes ROMP with the recently developed catalyst **4** which solves many problems of catalysts **1-3**. The first is described the living polymerization of norbornene and norbornene derivatives by catalyst **4** to produce polymers with very narrow polydispersity index (PDI) and good molecular weight control. It also promotes living ROMP of several monomers that previous catalysts had problems with. Lastly, syntheses of block copolymers are also described. In the second half of the chapter, ROMP of more challenging protic monomers are demonstrated. Amphiphilic block copolymers have been prepared by catalyst **4** which spontaneously undergo self-assembly into stable nanoparticles (10- 50 nm in radius) in non-hydrogen bonding solvents such as  $\text{CH}_2\text{Cl}_2$  and  $\text{CHCl}_3$ . Polymeric nanoparticles are characterized by NMR, GPC, DLS and SEM.

## Background

Ring-opening metathesis polymerization (ROMP) is one of the most used and studied chain growth polymerizations.<sup>1</sup> Unlike the step growth olefin polymerization, acyclic diene metathesis polymerization (ADMET),<sup>2</sup> ROMP is highly efficient for strained cycloalkenes because the metathesis equilibrium is shifted highly toward the ring opening process in order to release the ring strain. Over the last fifteen years, chemists have expanded the utility of ROMP by developing well-defined catalysts whose initiation and propagation can be controlled to produce well-defined polymers.<sup>3</sup> With the discovery of living polymerization of norbornenes to produce polymers with good molecular weight control and narrow PDI (eq 1),<sup>4</sup> ROMP was applied to many areas including electronic materials, electroluminescent material, packaging, solid support, and bioactive polymers.<sup>1</sup>

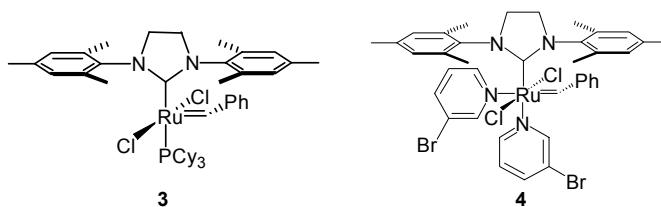


Recent advances include the efficient preparation of telechelic polymers (containing functionality at both ends of the polymer chains) with the highly active ruthenium catalyst,<sup>5</sup> and tandem polymerization with a single component ruthenium catalyst performing three mechanistically different catalyses in one pot (ROMP, atom transfer radical polymerization and hydrogenation).<sup>6</sup> The newest attraction in the field of ROMP is a modified ruthenium catalyst (cyclic catalyst or endless catalyst) producing high molecular weight cyclic polymers.<sup>7</sup> This polymerization represents the first general method to produce cyclic polymers with high yields and very low linear polymers contamination. In this chapter, living ROMP by the ultra-fast-initiating catalyst<sup>8</sup> and its application to the preparation of stable nanoparticles are described.

# Part I. Living Ring-Opening Metathesis Polymerization with an Ultrafast-initiating Ruthenium Catalyst

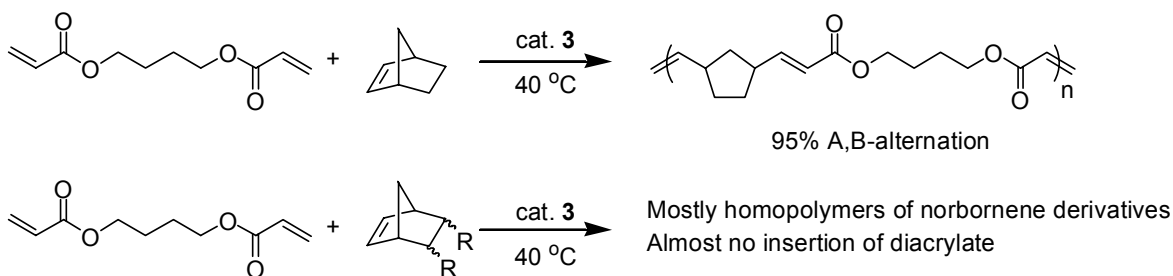
## Introduction

Ring-opening metathesis polymerization (ROMP) has expanded the realm of polymer synthesis, providing access to many structurally unique polymers.<sup>1</sup> With the development of well-defined olefin metathesis catalysts such as  $(t\text{-BuO})_2(\text{ArN})\text{-Mo=CH}(t\text{-Bu})$  (**1**)<sup>3</sup> and  $\text{Cl}_2(\text{PCy}_3)_2\text{Ru=CHPh}$  (**2**),<sup>9</sup> controlled living polymerizations became possible, making ROMP a novel method to synthesize polymers with various architectures. However, these catalysts suffer from either poor functional group tolerance (for **1**) or decreased activity and broader PDI (for **2**). The recently developed N-heterocyclic carbene ruthenium catalysts **3**<sup>10</sup> exhibits activity comparable to or higher than **1** while retaining the functional group tolerance of **2**. Catalyst **3** was found to be extremely useful in organic transformations, such as cross and ring-closing metathesis reactions.<sup>11</sup> However, **3** generally gives polymers with uncontrolled molecular weight and broad PDIs due to the high activity but slow initiation leading to incomplete initiation (small  $k_i/k_p$ )<sup>12</sup> and competing chain transfer reactions.<sup>5</sup>



From the previous study on ring opening-insertion metathesis polymerization (ROIMP),<sup>13</sup> we found that norbornene was a good comonomer, allowing to efficient insertion or chain transfer with diacrylates to yield A,B-alternating copolymers (Scheme 1). However, 2,3-disubstituted norbornenes were not viable comonomers since the steric hinderance around the olefin in the polymers prevented the required insertion of catalyst **3**. This suggested that chain transfer or back-biting was minimal even with the active catalyst **3** at 40 °C.<sup>14</sup> Recently a new member of the family of catalysts, **4**, has been found to initiate extremely rapidly, at least a

million times faster than **3**.<sup>15</sup> Therefore, increased  $k_i/k_p$  should promote living polymerization if chain transfer and chain termination reactions are absent. Herein, we report living ROMP of norbornene and 7-oxonorbornene derivatives by highly active and ultra-fast initiating ruthenium catalyst **4** to make monodisperse homopolymers and block copolymers.



Scheme 1. ROIMP of norbornene and norbornene derivatives

## Results and Discussion

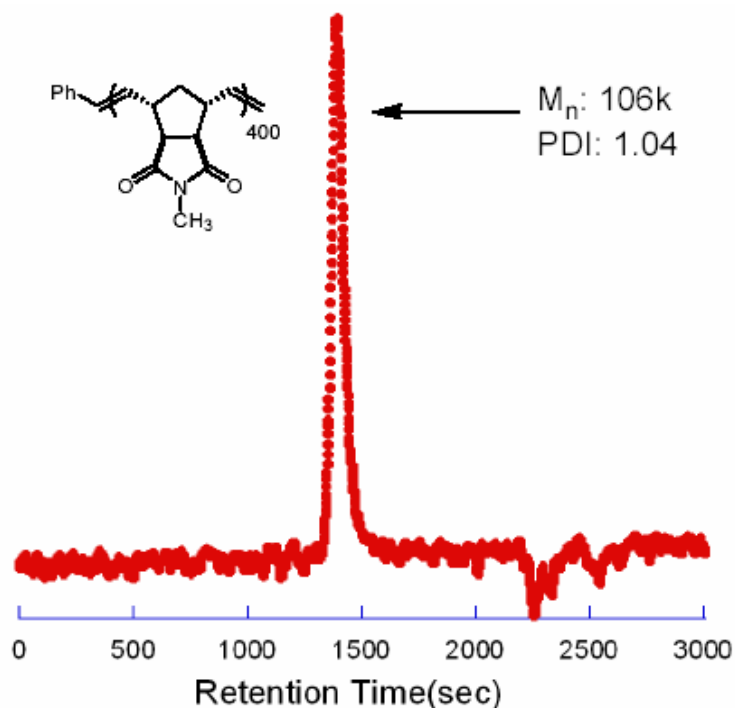
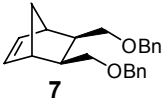
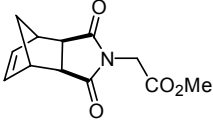
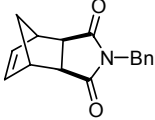
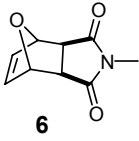
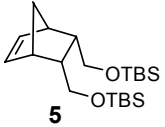
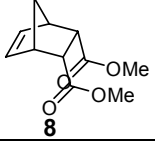
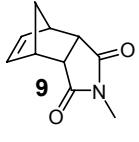
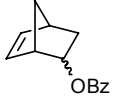


Figure 1. GPC trace of a narrow polydisperse polymer by catalyst **4**

Upon the addition of monomer solution to a solution of catalyst **4** in 0.2 – 0.4 M dichloromethane, the color instantaneously changes from green to yellow implying immediate

initiation of catalyst **4**. After 30 minutes, polymers were obtained by quenching the reactions with ethyl vinyl ether and precipitating them into methanol. As shown in Table 1, various polymers were obtained in high yields with PDIs as low as 1.04 (Figure 1 obtained by CH<sub>2</sub>Cl<sub>2</sub> GPC), which is indicative of controlled polymerization. It is worth noting that all the PDIs are much lower than typical controlled living ROMP products obtained from catalyst **2** ( PDI around 1.2). Also *endo*-monomers **8** and **9**, which polymerize slowly if at all with catalyst **2**, undergo ROMP readily with highly active catalyst **4**.<sup>9</sup> PDIs less than 1.10 for the ROMP polymers from *endo*-monomers are remarkably improved compared to PDI of 1.3 for the ROMP of *endo*-*N*-alkyl norbornene dicarboxyimides by catalyst **1**.<sup>16</sup>

Table 1. ROMP of various norbornene derivatives

monomer	M/C	obs. $M_n^a$ ( $\times 10^3$ )	theo. $M_n^b$ ( $\times 10^3$ )	PDI <sup>a</sup>
 <b>7</b>	100	30.4	33.5	1.05
	200	60.0	67.0	1.07
	400	131.5	133.9	1.06
 	100	27.5	23.6	1.04
	200	68.3	47.1	1.04
	400	134.5	94.2	1.04
 	100	53.1	18.0	1.04
	200	128.0	26.8	1.04
 <b>6</b>	100	29.1	18.0	1.05
	150	41.7	26.8	1.05
	200	53.1	35.9	1.06
	400	106.0	71.7	1.04
 <b>5</b>	100	24.5	38.3	1.06
	200	50.0	76.6	1.05
	400	114.0	153.1	1.04
 <b>8</b>	100	21.9	38.3	1.06
	200	63.7	76.6	1.06
 <b>9</b>	50	11.5	8.9	1.08
	100	22.9	17.8	1.08
	200	40.2	35.5	1.09
 	100	28.7	19.9	1.10
	200	50.6	39.7	1.10
	400	91.1	79.4	1.09

<sup>a</sup> Determined by CH<sub>2</sub>Cl<sub>2</sub> GPC relative to polystyrene standards.<sup>b</sup> Assuming quantitative conversion.

Encouraged by the narrow PDIs obtained with catalyst **4**, we examined the relationship between the molecular weight and monomer to catalyst ratio ( $[M]/[C]$ ). The representative graph of  $M_n$  versus  $[M]/[C]$  for monomers **6** and **7** is shown in Figure 2, which clearly shows a linear relationship between  $M_n$  and  $[M]/[C]$ . It is important to note that the linear relationship holds for

both low (as low as DP= 10) and high molecular weight polymers with narrow PDIs (< 1.1). Other monomers display similar linear relationships. The molecular weight control by  $[M]/[C]$  and the low PDIs suggest that for catalyst **4**,  $k_i/k_p$  is high enough that all the chains initiate and grow at a similar rate. The high  $k_i/k_p$  is attributed to the fact that although  $k_p$  of catalyst **4** is much larger than catalyst **2**, extremely high  $k_i$  (more than ten thousands times)<sup>12, 15</sup> overrides the increase in  $k_p$  relative to catalyst **2**, resulting in narrower PDI and good molecular weight control. Thus catalyst **4** promotes living ROMP with both higher activity and better control.

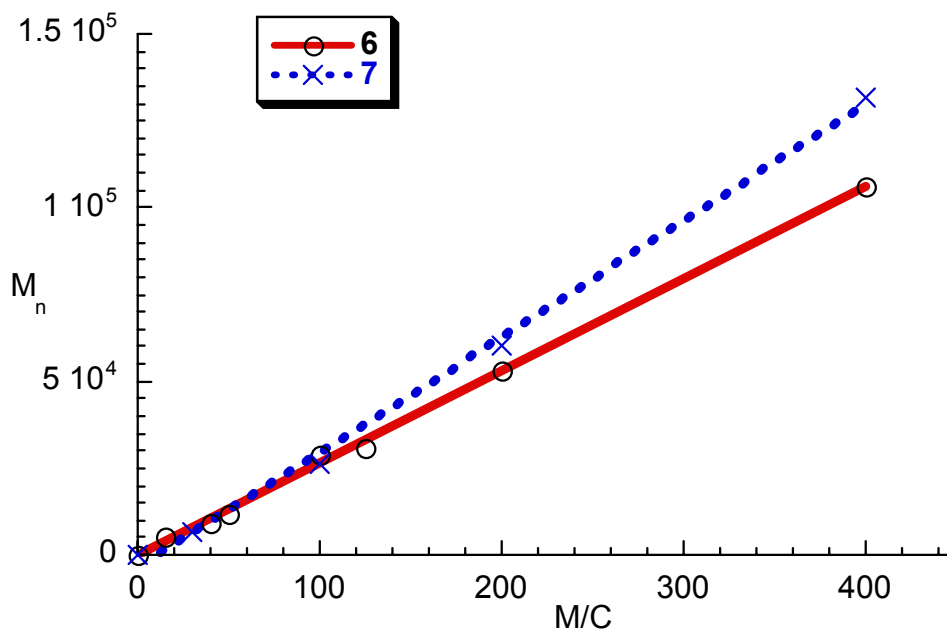


Figure 2. Relationship between  $M_n$  and  $[M]/[C]$  for monomers **6** and **7**

Table 2. Living ROMP of norbornene at -20 °C

M/C	obs. $M_n^a$ ( $\times 10^3$ )	theo. $M_n^b$ ( $\times 10^3$ )	PDI <sup>a</sup>
50	4.4	4.8	1.08
100	9.0	9.5	1.09
150	15.1	14.2	1.06
200	22.0	18.9	1.10

<sup>a</sup> Determined by CH<sub>2</sub>Cl<sub>2</sub> GPC relative to polystyrene standards. A correction factor of 0.5 applied <sup>b</sup> Assuming quantitative conversion.



Norbornene is a unique monomer since only catalyst **1** and  $\text{Cl}_2(\text{PPh}_3)_2\text{Ru}=\text{CHPh}$ ,<sup>9b</sup> promote living polymerization. Catalyst **2** and **3** give broad PDI (around two) for polynorbornene (PNB) due to chain transfer reactions.<sup>5b, 9b</sup> Not surprisingly, **4** also produced (PNB) with broad PDI of 1.65 at room temperature. However, PNB with narrower PDI (1.28) was obtained when the polymerization was run at 0 °C and finally PDI was further decrease to 1.08 when the polymerization was run at -20 °C. It is notable that **4** initiates rapidly even at -20 °C, and the low PDI indicates that chain transfer reactions on PNB are suppressed at low temperatures. Furthermore, good molecular weight control by varying  $[\text{M}]/[\text{C}]$ . Close matching of observed  $M_n$  and theoretical  $M_n$  showed that catalyst **4** could also promote living ROMP of norbornene at -20 °C (Table 2, and Figure 3).

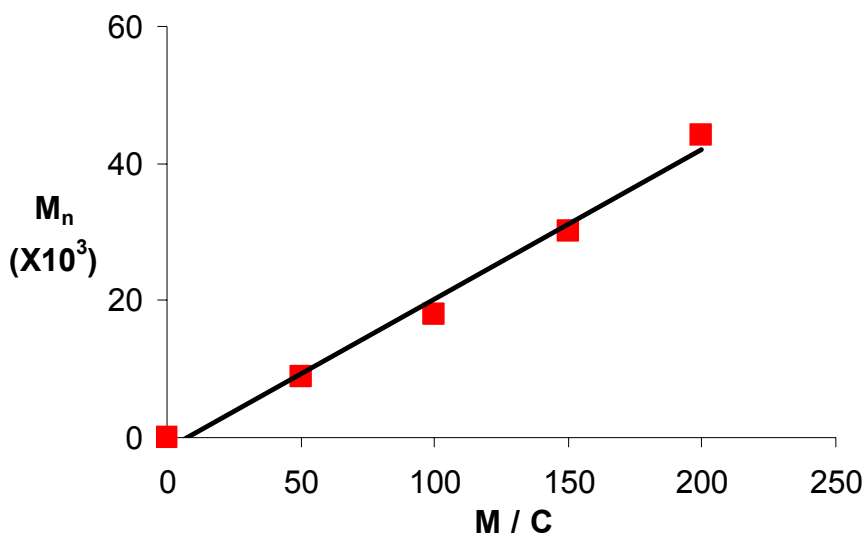


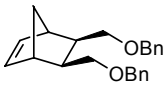
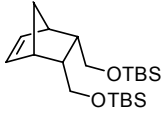
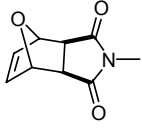
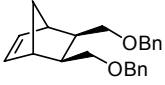
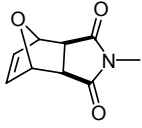
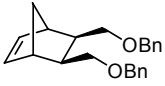
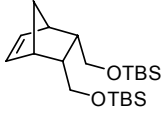
Figure 3. Relationship between  $M_n$  and  $[\text{M}]/[\text{C}]$  for norbornene

The effects of changing the polymerization conditions were studied using 100 equivalents of monomer **6** relative to catalyst **4**. Lowering the reaction concentration to 0.05 M in dichloromethane or lowering the temperature to 0 °C had no effects on the isolated yields, molecular weights, or PDI. Changing to different solvents had no marked effects, but raising the temperature from 23 °C to 55 °C in 1,2-dichloroethane gave a polymer with similar  $M_n$  but much

broadener PDI of 1.25. This suggests that chain transfer or back-biting does occur at higher temperatures.<sup>5a</sup>

If catalyst **4** indeed promotes the controlled living polymerization of norbornenes and 7-oxonorbornene derivatives, it should produce block copolymers from sequential additions of monomer. Monomer **7** (200 equivalents) was treated with catalyst **4** followed by the addition of monomer **5** (200 equivalents) after 30 minutes (Table 3, entry 1). The final polymer with about twice  $M_n$  of initial homopolymer **7** and PDI of 1.10 was obtained.  $^1\text{H}$  NMR spectrum showed only two sets of overlaying peaks identical to those of two homopolymers. To show that the product was truly a diblock copolymer, another block copolymer was synthesized using 50 equivalents of monomer **6** followed by 200 equivalents of monomer **7**. Figure 4a clearly shows well resolved GPC traces for the diblock copolymer of entry 2 (Table 3) where the signal of the first monomer is wholly shifted to higher molecular weight region. The  $M_n$  value of the final copolymer (73k) agrees with the sum of the  $M_n$ s of individually synthesized homopolymers of **6** and **7** (10k + 60k = 70k). ABC-Triblock copolymers by sequential addition of three different monomers (entry 3) can be also made. Figure 4b displays well resolved GPC traces of for the narrow polydisperse triblock copolymer. No fractions are observed in the low molecular weight regions indicating that no termination occurred during the course of the two sequential additions of monomers. In all cases, the observed ratios of the monomers by  $^1\text{H}$  NMR of the final block copolymers are in good agreement with the added feed ratios.

Table 3. Synthesis of block copolymers<sup>a</sup>

entry	1 <sup>st</sup> monomer	M/C	M <sub>n</sub> <sup>b</sup> (X 10 <sup>3</sup> )	2 <sup>nd</sup> monomer	M/C	M <sub>n</sub> <sup>b</sup> (X 10 <sup>3</sup> )	yield [%]	PDI <sup>b</sup>
1		200	60.6		200	115.1	90	1.10
2		50	10.0		200	72.7	86	1.07
3		15	5.1		75	37.4	-	1.06
			3 <sup>rd</sup> monomer		370	154.8	90	1.05

<sup>a</sup> 0.2 M in CH<sub>2</sub>Cl<sub>2</sub> at 23 °C 30 min for each monomer. <sup>b</sup> Determined by CH<sub>2</sub>Cl<sub>2</sub> GPC relative to polystyrene standards.<sup>c</sup> Yield of product isolated by precipitation into methanol.

## Conclusion

In this section, we have demonstrated that catalyst **4**, bearing an N-heterocyclic carbene which greatly enhances the activity and 3-bromopyridine ligands which increase the initiation rate tremendously, shows controlled living polymerization of norbornene and oxo-norbornene derivatives. Catalyst **4** expands the substrate scope including those that do not show living polymerization with the previous catalysts. Block copolymers were also successfully prepared.

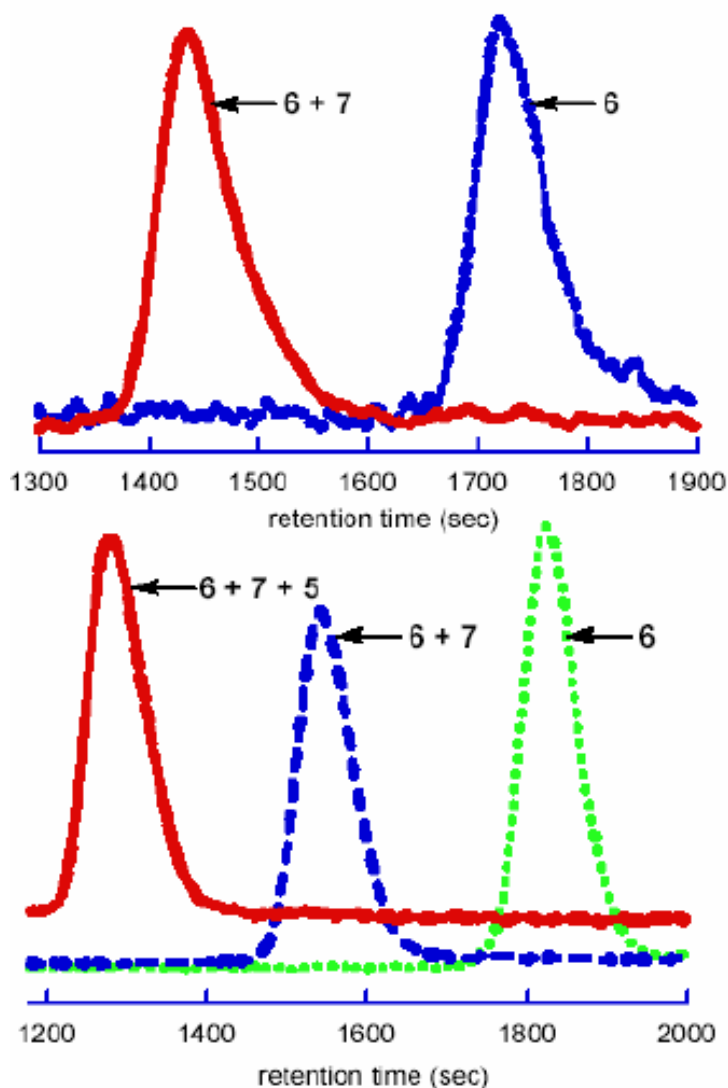


Figure 4. GPC traces of di- and triblock copolymers

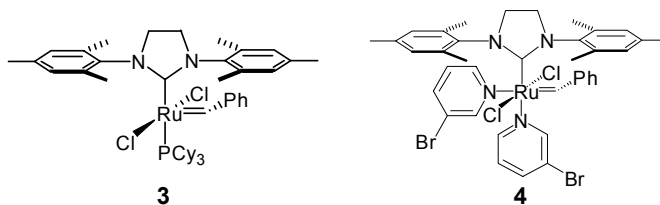
## Part II. Mild Synthesis of Polymeric Nanoparticles by Living ROMP

### Introduction

Polymeric micelles have attracted great attention due to their novel structures resembling dendrimers<sup>17</sup> and their potential applications towards drug delivery<sup>18</sup> and supporting catalysts.<sup>19</sup> Generally, polymeric micelles are prepared from block copolymers in selective solvents, where the solvent acts as a good solvent for one block (shell) and a bad solvent for the other block resulting in self-assembly to make a core. From the resulting polymeric micelles, polymeric

nanoparticles are prepared by covalently cross-linking the core<sup>20</sup> or the shell.<sup>21</sup> Many methods exist for the synthesis of core-shell micelles and nanoparticles, but a more functional group tolerant, user friendly, and milder method exhibiting good control on particle sizes would be valuable.

Ring-opening metathesis polymerization (ROMP) has expanded the realm of polymer synthesis.<sup>1</sup> With the developments of well-defined olefin metathesis catalysts such as (t-BuO)<sub>2</sub>(ArN)-Mo=CH(*t*-Bu) (**1**)<sup>3</sup> and Cl<sub>2</sub>(PCy<sub>3</sub>)<sub>2</sub>Ru=CHPh (**2**),<sup>9</sup> living polymerization became possible, making ROMP a novel method to synthesize polymer with various architectures. However, these catalysts suffer from either lack of the functional group tolerance (**1**) or the decreased activity and relatively broader polydispersity of 1.2 (**2**). Recently developed N-heterocyclic carbene ruthenium catalyst **3**,<sup>10</sup> solved some of the problems by exhibiting activity comparable to or higher than **1** while retaining the functional group tolerance of **2**. However, **3** has drawbacks such as poor molecular weight control and broad PDIs.<sup>5a</sup>

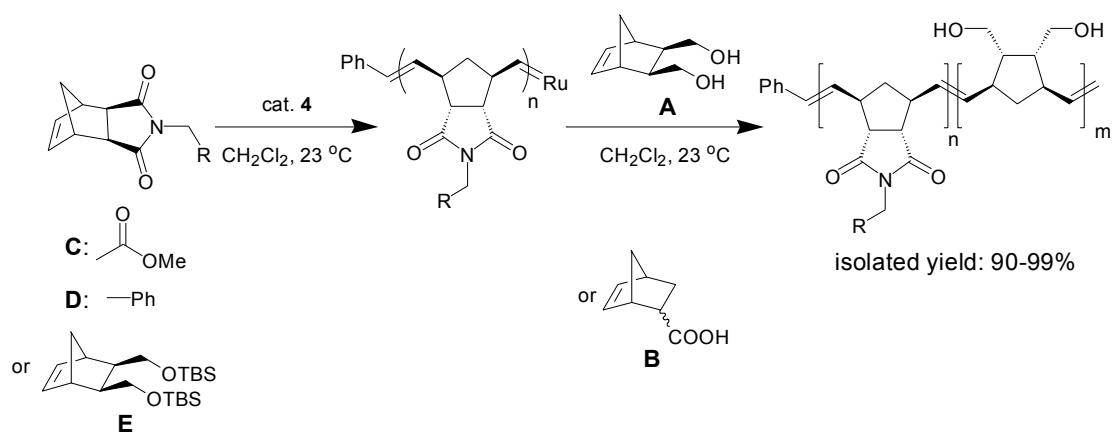


The most recent development of ultra-fast initiating ruthenium catalyst **4**<sup>15</sup> showed improvements over the previous catalysts by exhibiting high activity but still retaining the functional group tolerance of **2** and producing polymers with narrow polydispersity less than 1.1.<sup>8</sup> Herein we report a convenient and mild synthesis of diblock copolymers by ROMP by **4** which self-assemble into stable core-shell nanoparticles even without cross-linking.

## Results and Discussion

Previous report from our group showed that catalyst **4** produced di- and triblock copolymers with narrow PDI by living ROMP (Part I of this chapter).<sup>8</sup> With this catalyst in hand,

we tried ROMP of protic monomers that had not been reported in the literature (for example, 5-norbornene-2-*exo*,3-*exo*-dimethanol (**A**) and 5-norbornene-2-carboxylic acid (**B**)). As soon as monomer **A** was added to a CH<sub>2</sub>Cl<sub>2</sub> solution of catalyst **4**, ROMP polymer immediately precipitated out of the reaction solution. The resulting polymer, which was insoluble in CH<sub>2</sub>Cl<sub>2</sub>, but soluble in DMSO, had an average degree of polymerization (DP) of 20. Another monomer with a protic functional group, 5-norbornene-2-carboxylic acid (**B**) also showed similar result as monomer **A**. These results implied that catalyst **4** is tolerant of protic functional groups such as alcohols, diols and carboxylic acids functional groups. Encouraged by these results, we pursued the synthesis of diblock copolymers whereby one monomers would produce a block well solvated by the reaction solution, CH<sub>2</sub>Cl<sub>2</sub> (**C**- **E**), and the other, protic monomers capable of hydrogen bond (**A** and **B**).



advantages of the ROMP procedure is the mild conditions, such as room temperature, bench-top reaction where no rigorous techniques or equipment are required and short reaction time typically less than an hour. Also, due to the living nature, the DP of each block can be easily controlled by changing the monomer to catalyst ratio.

Characterizing the block copolymers by NMR spectroscopy provides insight into the polymer's structure. For example, a block copolymer of monomers **A** and **C** was examined by  $^1\text{H}$  and  $^{13}\text{C}$  NMR in  $\text{CDCl}_3$  and spectra showed only one set of peaks corresponding to homopolymer of **C** and none for the block corresponding to **A** (Figure 5). However, when dissolved in a hydrogen bonding solvent such as  $\text{DMSO}_{\text{d-6}}$ , which is a good solvent for both block, all of the peaks expected for both blocks were visible by  $^1\text{H}$  and  $^{13}\text{C}$  NMR (Figure 6). Solid state NMR further confirmed the presence of both blocks. Furthermore, a gradual appearance of broad peaks corresponding to the diol block **A** was noticed when a small amount of  $\text{DMSO}_{\text{d-6}}$  was added to the polymer solution in  $\text{CDCl}_3$  and finally, the new peaks sharpened at 9% by volume  $\text{DMSO}_{\text{d-6}}$ . The similar broad peaks for the diol block were observed in another hydrogen bonding solvent  $\text{THF}_{\text{d-8}}$  at room temperature and at  $60\text{ }^\circ\text{C}$ , the peaks sharpened again. These observations suggest that the diblock copolymer was undergoing some type of aggregation such as a core-shell micelle formation where methylene chloride and chloroform act as selective solvents for blocks **C** (shell) and bad solvents for **A** (core). Therefore the peaks for the non-solvated, thus self-assembled core **4** with low mobility, can be regarded as semi-solid whose peaks greatly broaden and disappear in NMR spectra,<sup>22</sup> whereas in  $\text{DMSO}_{\text{d-6}}$  all the peaks for the block copolymer are observed. Apparently, diol functionality in the second block provides strong driving force for the self-assembly process. As a result, a small amount of hydrogen bond breaking  $\text{DMSO}_{\text{d-6}}$  added to the  $\text{CDCl}_3$  solution of the block copolymer can efficiently disrupts the self-assembly.

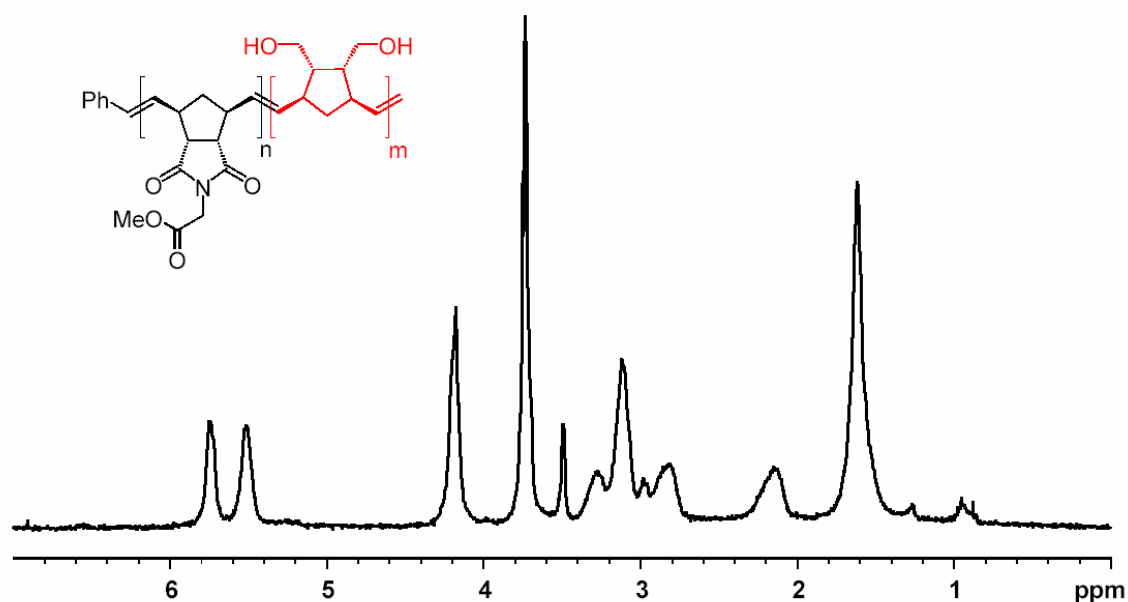


Figure 5.  $^1\text{H}$  NMR spectrum for an amphotiphilic block copolymer in  $\text{CDCl}_3$

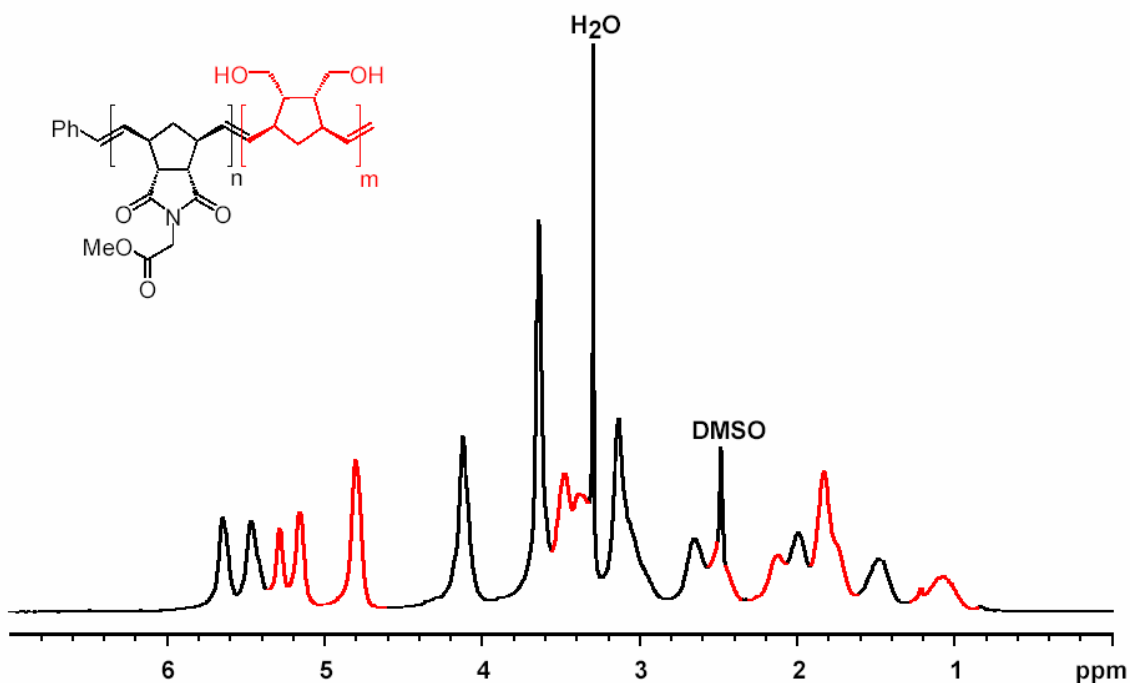


Figure 6.  $^1\text{H}$  NMR spectrum for an amphotiphilic block copolymer in  $\text{DMSO}_{d-6}$

Molecular weight analysis by GPC using non-hydrogen bonding  $\text{CH}_2\text{Cl}_2$  mobile phase strongly supports the formation of hydrogen-bonded self-assembled supramolecules. GPC analysis of a diblock copolymer shown in Figure 7 shows majority of high molecular weight



material (nearly  $1.3 \times 10^6$  g/mol) and a minor fraction of low molecular weight material (26,000 g/mol). Since the theoretical  $M_n$  of the block copolymer is about 31,000 g/mol, the self-assembled supramolecule formation must be responsible for the major high molecular weight trace while the minor peak corresponds to the homopolymer of **C**. The high molecular weight polymer is not due to cross-linking or other covalent bond formation because GPC analysis eluted by THF shows a major trace at low molecular weight. Also, a random copolymer of 1: 1 mixture of **C** and **A** prepared by catalyst **4** shows a major trace at low molecular weight fraction. It is notable that the self-assembled diblock copolymers are so tightly bound that supramolecules are not dissociated under the shear pressures of GPC condition. In other words, if the binding force of the self-assembly were weak, or in dynamic equilibrium as in micelles, GPC analysis would show a major trace corresponding to a single polymer chain. The observation of such high molecular weight supramolecules by GPC implies that the diblock copolymers undergo self-assembly to form stable polymeric nanoparticles even without covalent cross-linking. The stability of the polymeric nanoparticles is likely due to the strong interchain hydrogen bonding from the protic blocks which collapse into well-organized cores of the nanoparticles. For the random copolymer, such a strong association between the polymer chains is less likely since the self-assembling protic monomers are randomly incorporated into the polymer chains, thus the interaction of the dispersed hydrogen bond is weak. Also, no stable nanoparticle was observed by GPC analysis (the absence of high molecular weight trace) for the diblock copolymers with DP of the diol block **A** less than 15, as fewer numbers of hydrogen-bond interactions weakens the self-assembling interaction.

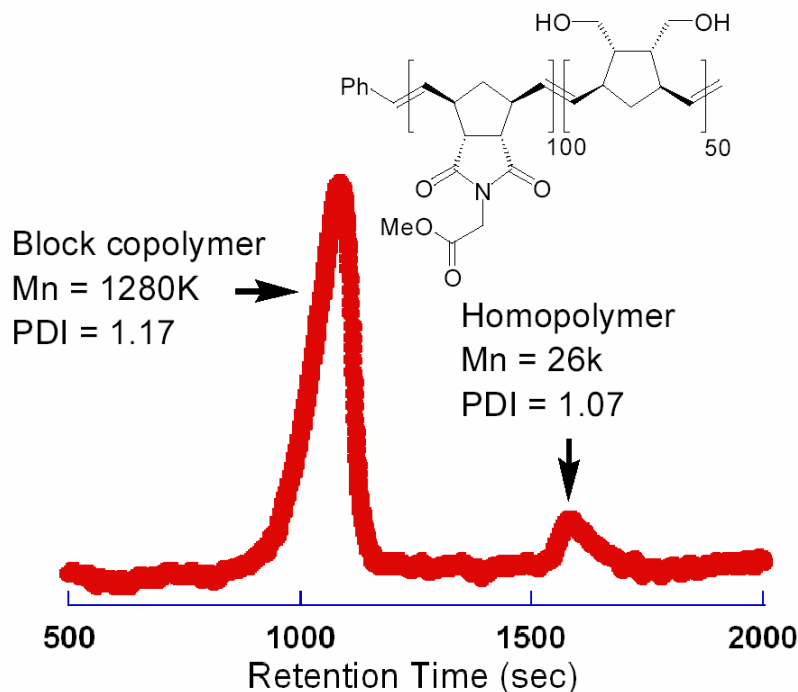


Figure 7. GPC traces of stable supramolecules eluted by  $\text{CH}_2\text{Cl}_2$

To examine the dimensions of the self-assembled nanoparticles in  $\text{CH}_2\text{Cl}_2$  solution, dynamic light scattering (DLS) was used to measure hydrodynamic radius ( $R_h$ ) of the nanoparticles. DLS analysis was conducted with 0.015 wt% of block copolymers in  $\text{CH}_2\text{Cl}_2$  at 20 °C. Representative DLS data for a self-assembled block copolymer of **C** (100eq) and **A** (25eq) is plotted in Figure 8 showing almost monodisperse distribution (polydispersity of 0.03) of particle size with  $R_h$  of 23.6 nm. Other block copolymers from difference monomers with various composites were synthesized and their DLS data are listed in Table 4 showing  $R_h$  values ranging from 10 to 50 nm and narrow distribution of the particle sizes (polydispersity below 0.09). As expected from the living nature of ROMP by catalyst **4**, the sizes of the nanoparticles increase with the larger DP of the each block. Therefore, the nanoparticle sizes can be easily controlled by changing the monomer to catalyst ratio during the synthesis of the diblock copolymers. The narrow polydispersity (below 0.1) of the particle sizes calculated by DLS reflects the ability of catalyst **4** to produce polymers with narrow PDI. It is quite remarkable that low molecular weight diblock copolymers with a total DP of 30 can self-assemble into the stable nanoparticles (Table 4,

entry 1).

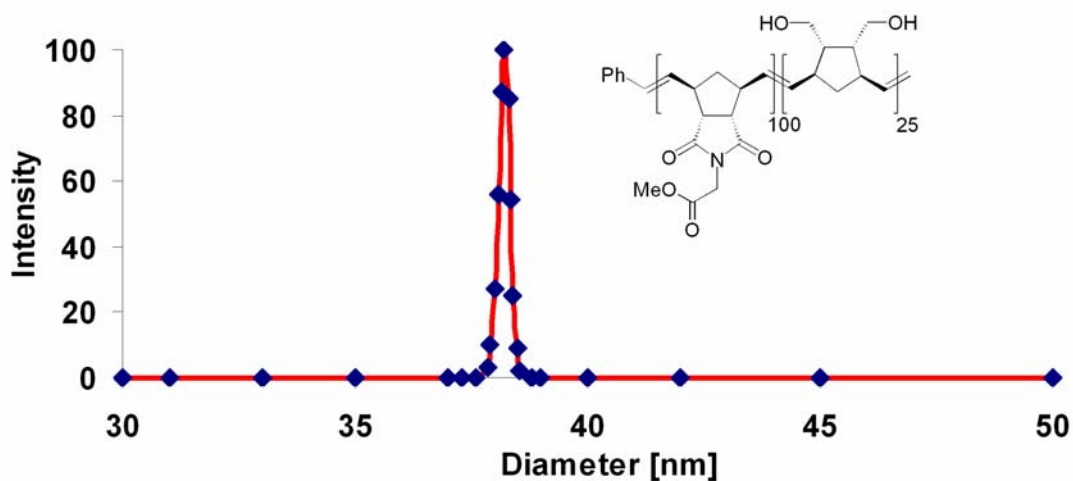
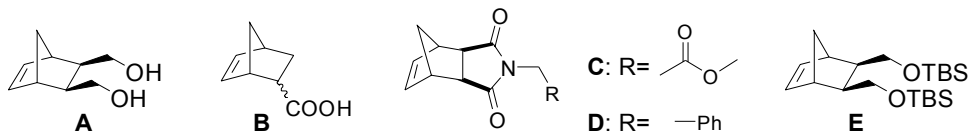


Figure 8. DLS analysis to show  $R_h$  in solution

Table 4. DLS data for various polymeric nanoparticles

entry	1 <sup>st</sup> block (DP)	2 <sup>nd</sup> block (DP)	$M_n$ (PDI) <sup>a</sup>	$R_h$ [nm] <sup>b</sup>	polydispersity <sup>b</sup>
1	<b>C</b> (10)	<b>A</b> (20)	508K (1.75)	10.9	0.04
2	<b>C</b> (25)	<b>A</b> (25)	919K (1.47)	13.3	0.02
3	<b>C</b> (50)	<b>A</b> (25)	1170K (1.32)	19.1	0.03
4	<b>C</b> (100)	<b>A</b> (25)	1100K (1.12)	23.8	0.03
5	<b>C</b> (100)	<b>A</b> (50)	1280K (1.17)	27.5	0.01
6	<b>D</b> (35)	<b>A</b> (35)	1300K (1.42)	16.1	0.05
7	<b>D</b> (100)	<b>A</b> (50)	1350K (1.11)	33.1	0.05
8	<b>E</b> (50)	<b>A</b> (25)	747K (1.11)	18.7	0.06
9	<b>E</b> (100)	<b>A</b> (50)	1880K (1.15)	34.3	0.02
10	<b>C</b> (20)	<b>B</b> (20)	1300K (2.00)	16.0	0.05
11	<b>E</b> (100)	<b>B</b> (30)	967K (1.31)	47.9	0.09

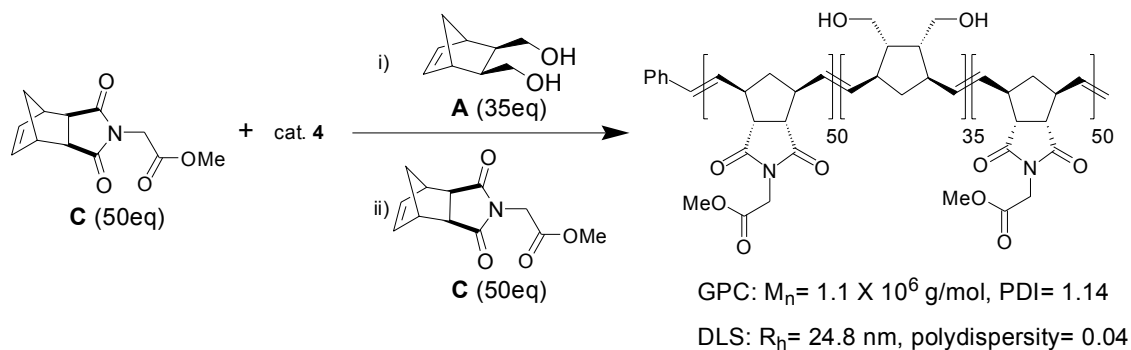
<sup>a</sup>  $\text{CH}_2\text{Cl}_2$  GPC relative to PS standard <sup>b</sup> Determined by DLS, 0.015 wt % in  $\text{CH}_2\text{Cl}_2$



Concentration effects of the nanoparticles on particle sizes were also investigated. A diblock copolymer from **C** (50) and **A** (25) (Table 4, entry 3) was dissolved in three different concentrations, 0.015 wt%, 0.15 wt% and 0.75 wt% and their  $R_h$  were measured to be 19.1 nm, 16.3 nm and 13.2 nm respectively. Slight decrease in particle sizes (30%) with retained narrow size distributions was observed with large increases (50 times) in the concentration. Compared to micelles where size is highly concentration dependent, concentration effect for the polymeric nanoparticles is less significant. Slight decrease in particle sizes may be due to the perturbations in viscosity and refractive index, to which DLS measurements are sensitive, during the large changes in concentrations.

Not surprisingly, homopolymers of **C** and **D** gives poor DLS data because small particles of single random coils are poor scatters of light. Also the block copolymers dissolved in hydrogen-bonding solvents such as DMSO and THF responded poorly by DLS analysis, indicating that the hydrogen-bonding driven self-assembly was disrupted. These observation along with NMR and GPC analysis, strongly support that the amphiphilic diblock copolymers undergoes self-assembly into stable nanoparticles in non-hydrogen bonding solvent, but are disassembled into random coils in hydrogen-bonding solvents.

A triblock copolymer was synthesized with the similar procedure (Scheme 3). The resulting polymer behaved similarly to the diblock copolymers, showing a high molecular weight trace ( $M_n = 1.1 \times 10^6$  g/mol) by  $\text{CH}_2\text{Cl}_2$  GPC and an  $R_h$  of 24.8 nm with narrow polydispersity by DLS analysis. Triblock copolymers can be more advantageous since they can contain more functionality compared to diblock copolymers.



Scheme 3. Preparation of nanoparticles from a triblock copolymer

Solid-state structures of polymeric nanoparticles were visualized by high-resolution scanning electron microscopy (SEM). A small amount of powder of the diblock copolymer was mounted on the carbon tape. Shown in Figure 9 is the polymeric nanoparticles from **E** (100) and **A** (50) obtained after precipitation into hexane (Table 4 entry 9). Sphere-like nanoparticles of around 40 nm in diameter can be identified by SEM analysis. Typically the sizes for the solid state (eg. 40 nm) is smaller than that obtained by a solution method, such as DSL (eg. 69 nm) because well solvated polymers tend to swell in solution, giving larger sizes.

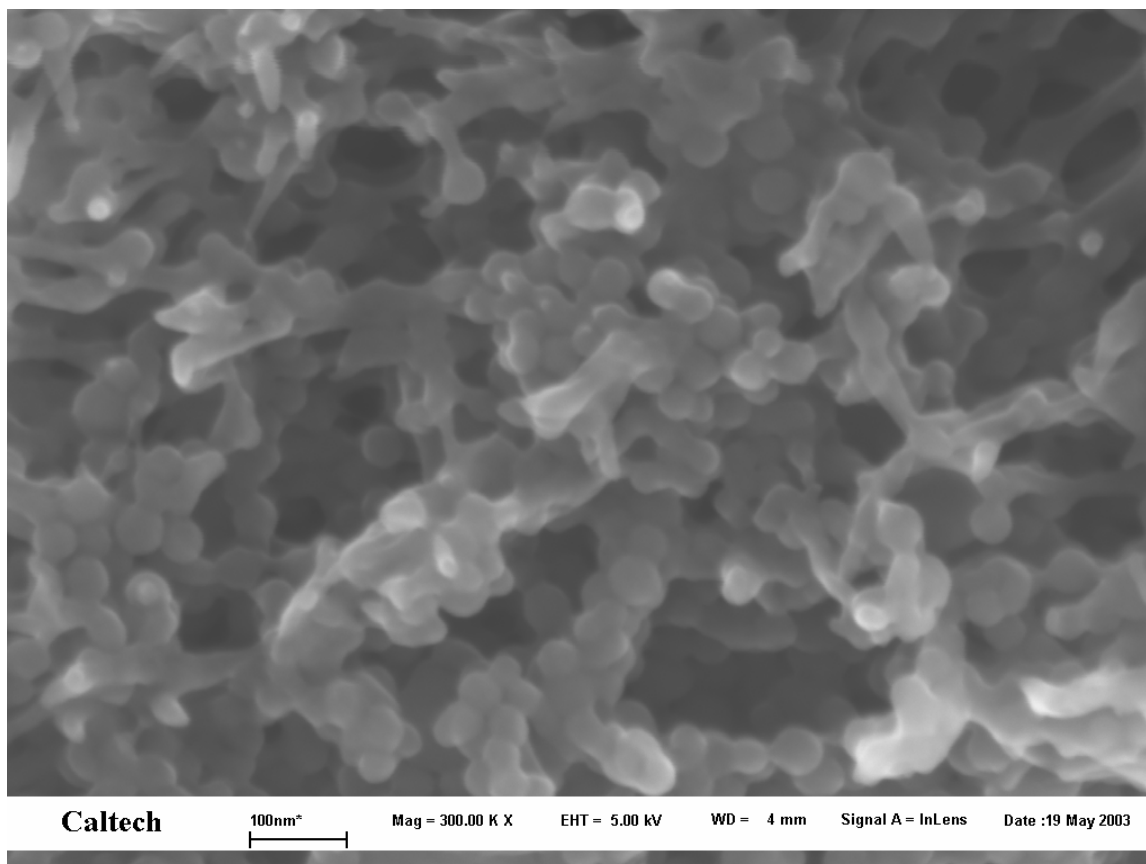


Figure 9. SEM image of polymeric nanoparticles

When a dilute  $\text{CH}_2\text{Cl}_2$  solution of the nanoparticles prepared from **C** (20) and **B** (20) (Table 4, entry 10) was cast onto the surface of a silicon wafer and dried in humid air, a film of honey-comb structures was obtained as visualized by SEM (Figure 10). The well-ordered honey-comb with 1  $\mu\text{m}$  pore and 250 nm thick walls can be observed. It has been proposed that when a film of polymers is casted in humid air, solvent evaporates and water droplets condense in the film to form honey-comb structure (Figure 11).<sup>23</sup> It seems that self-assembled block copolymer solution improves the quality of the honey-comb structures since the film cast by homopolymers or conventional block copolymers produce poorly ordered structure.

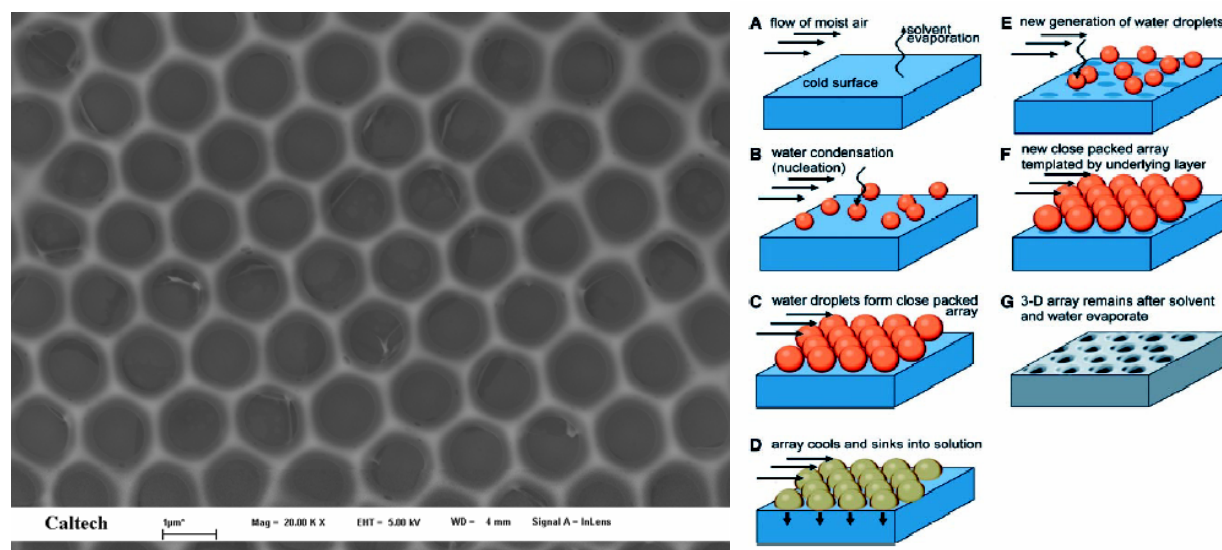


Figure 10. SEM image of honey-comb structures and the proposed mechanism of formation

## Conclusion

We have demonstrated that catalyst **4** can be used to synthesize diblock and triblock copolymers that spontaneously self-assemble into stable nanoparticles. Living ROMP allows the preparation of the polymeric nanoparticles under mild conditions with good control of the particle sizes by varying the monomers to catalyst ratio for each block. Nanoparticles with  $R_h$  as low as 10.9 nm and narrow size distribution were prepared. NMR experiments gave the indication of self-assembly process, DLS provided information on the sizes and size distribution of the particles in solution, and GPC analysis showed that the hydrogen-bond-driven self-assembly yields stable polymeric nanoparticles. Finally, visualization of the nanoparticles in the solid state was possible by SEM.

**Acknowledgements.** I would like to thank the NSF for generous support of this research, and Prof. K. L. Wooley, Dr. C. Bielawski, Dr. J. S. Kim, S. Y. Lee, Isaac M. Rutenberg, Oren A. Scherman and S. R. Popielarski for helpful discussion and instrumental help.

## Experimental Section

**Instrumentation.** NMR spectra were recorded on Varian Mercury-300 NMR (300 MHz for  $^1\text{H}$  and 74.5 MHz for  $^{13}\text{C}$ ). Chemical shifts are reported in parts per million (ppm) downfield from tetramethylsilane (TMS) with reference to internal solvent. Multiplicities are abbreviated as follows: singlet (s), doublet (d), triplet (t), quartet (q), quintet (quint), and multiplet (m). The reported  $^1\text{H}$  NMR data refer to the major olefin isomer unless stated otherwise. The reported  $^{13}\text{C}$  NMR data include all peaks observed and no peak assignments were made. Gel permeation chromatography (GPC) analysis in  $\text{CH}_2\text{Cl}_2$  was obtained on a HPLC system using a Shimadzu LC-10AP<sub>vp</sub> pump, Shimadzu DGU-14A degasser, a Rheodyne model 7125 injector with a 100  $\mu\text{l}$  injection loop through Polymer Standard 10 micron mixed bed columns, and a Knauer differential-refractometer. Molecular weights and molecular weight distributions,  $M_w/M_n$ , are reported relative to narrow disperse polystyrene standards (Showa Denko). Another GPC system was eluted by THF through two PLgel 5 mm mixed-C columns (Polymer Labs) connected in series with a DAWN EOS multiangle laser light scattering (MALLS) detector and an Optilab DSP differential refractometer both from Wyatt Technology. The  $dn/dc$  values were obtained for each injection assuming 100% mass elution from the columns. Dynamic light scattering (DLS) data was obtained from Brookhaven 90Plus using ZetaPALS particle sizing software. High resolution SEM images were obtained from LEO 1550VP.

**General Procedure for ROMP of norbornenes:** To a vial charged with a solution of catalyst **4** in 1 ml of  $\text{CH}_2\text{Cl}_2$  under argon atmosphere, a solution of monomers in 0.5 ml of  $\text{CH}_2\text{Cl}_2$  was added rapidly via syringe at room temperature. Quick degassing by dynamic vacuum was conducted. After 30 minutes, the reaction was quenched by addition of excess ethyl vinyl ether. The polymer product was obtained by precipitation into methanol, and dried overnight.

**Procedure for ROMP of monomer 7:** To a vial charged with catalyst **4** (1.0 mg, 1.1  $\mu\text{mol}$ ) in 1



ml of CH<sub>2</sub>Cl<sub>2</sub> under argon atmosphere, solution of **7** (150 mg, 0.45 mmol) in 0.5 ml of CH<sub>2</sub>Cl<sub>2</sub> was added rapidly via syringe at room temperature. After 30 minutes, the product (135 mg, 90% yield, 59% *cis* olefin) was obtained by precipitation into methanol. <sup>1</sup>H NMR (300MHz, CDCl<sub>3</sub>, ppm): δ 7.25 (10H, bs), 5.25 (2H, bm), 4.30 (4H, bm), 3.45 (4H, bs), 2.76 (1.2H for *cis*, bs), 2.38 (0.8H for *trans*, bs), 2.03 (3H, bm), 1.12 (1H, bs). <sup>13</sup>C NMR (75 MHz, CDCl<sub>3</sub>, ppm): δ 138.9(b), 134.0(b), 128.5, 127.7, 127.6, 73.2, 70.7, 70.4, 48.0, 47.7, 45.4 (bm), 41.3 (bm), 40.3. Other homopolymers are all known and well characterized.<sup>9</sup>

**Procedure for ROMP of monomer A:** To a vial charged with catalyst **4** (2.6 mg, 2.9 μmol) in 1 ml of CH<sub>2</sub>Cl<sub>2</sub> under argon atmosphere, solution of **A** (22.5 mg, 0.15 mmol) in 0.5 ml of CH<sub>2</sub>Cl<sub>2</sub> was added rapidly via syringe at room temperature. Immediately, the product (14 mg, 62% yield, 56% *cis* olefin) was obtained. <sup>1</sup>H NMR (300MHz, DMSO<sub>d-6</sub>, ppm): δ 5.27 (0.9H for *trans*, bs), 5.15 (1.1H for *cis*, bs), 4.83 (2H, bs), 3.44 (4H, br), 2.45 (1.1H for *cis*, bs), 2.10 (0.9H for *trans*, bs), 1.82 (3H, bm), 1.07 (1H, bm).

**Procedure for ROMP of monomer B:** To a vial charged with catalyst **4** (3.4 mg, 3.9 μmol) in 1 ml of CH<sub>2</sub>Cl<sub>2</sub> under argon atmosphere, solution of **A** (23 mg, 0.15 mmol) in 0.5 ml of CH<sub>2</sub>Cl<sub>2</sub> was added rapidly via syringe at room temperature. Immediately, the product (14 mg, 61%,) was obtained. <sup>1</sup>H NMR (300MHz, CD<sub>3</sub>OD, ppm): δ 5.35 (2H, bm), 2.9 (1H, bm), 2.52 (1H, bm), 1.98 (2H, bm), 1.7 (1H, bm), 1.3 (1H, bm).

**Representative Procedure for amphiphilic diblock synthesis:** To a vial charged with catalyst **4** (2.0 mg, 2.3 μmol) in 0.5 ml of CH<sub>2</sub>Cl<sub>2</sub> under argon atmosphere, solution of **D** (57 mg, 0.23 mmol) in 0.5 ml of CH<sub>2</sub>Cl<sub>2</sub> was added rapidly at room temperature. After 20 minutes, another solution of **A** (18 mg, 0.12 mmol) in 0.5 ml of CH<sub>2</sub>Cl<sub>2</sub> was added rapidly. After 30 minutes, ROMP was quenched by addition of excess ethyl vinyl ether. The product (73 mg, 98%) was obtained by precipitation into methanol and drying on vacuum pump for overnight. <sup>1</sup>H NMR (300MHz, DMSO<sub>d-6</sub>, ppm): δ 7.20 (5H, bs), 5.61 (0.8H for *trans*, bs), 5.43 (1.2H for *cis*, bm), 5.29 (0.8H for

trans, bs), 5.15 (1.2H for cis), 4.81 (2H, bs), 4.46 (2H, bm), 2.50- 3.35 (4H, bm), 1.0- 2.0 (6H, bm). <sup>13</sup>C NMR (75 MHz, DMSO<sub>d-6</sub>, ppm): δ 178.6, 178.3, 136.9, 134.3, 133.7, 132.8, 132.1, 129.1, 128.0, 61.1, 53.1, 52.6, 51.3, 50.7, 49.5, 45.6, 42.0. 40 (br).

## Reference:

1. For recent reviews on ROMP, see: a) Novak, B. M.; Risse, W.; Grubbs, R. H. *Adv. Polym. Sci.* **1992**, *102*, 47; b) Ivin, K. J.; Mol, J. C. *Olefin Metathesis and Metathesis Polymerization*, Academic Press, San Diego, CA, **1997**; c) Grubbs, R. H.; Khosravi, E. *Material Science and Technology*, **1999**, *20*, 65; d) Buchmeiser, M. R. *Chem. Rev.* **2000**, *100*, 1565.
2. Lehman, S. E.; Wagener, K. B. *Macromolecules* **2002**, *35*, 48.
3. a) Schrock, R. R. *Acc. Chem. Res.* **1990**, *23*, 158; b) Bazan, G. C.; Schrock, R. R.; Cho, H. N.; Gibson, V. C. *Macromolecules* **1991**, *24*, 4495.
4. Grubbs, R. H.; Tumas, W. *Science* **1989**, *243*, 907
5. a) Bielawski, C. W.; Grubbs, R. H. *Angew. Chem, Int. Ed.* **2000**, *39*, 2903; b) Bielawski, C. W.; Benitez, D.; Grubbs, R. H. *Macromolecules* **2001**, *34*, 8610; c) Scherman, O. A.; Kim, H. M.; Grubbs, R. H. *Macromolecules* **2002**, *35*, 5366.
6. Bielawski, C. W.; Louie, J.; Grubbs, R. H. *J. Am. Chem. Soc.* **2000**, *122*, 2872.
7. a) Bielawski, C. W.; Benitez, D.; Grubbs, R. H. *Science* **2003**, *297*, 2041; b) Bielawski, C. W.; Benitez, D.; Grubbs, R. H. *J. Am. Chem. Soc.* **2003**, *125*, 8424.
8. This portion of the work is published; Choi, T.-L.; Grubbs, R. H. *Angew. Chem. Int. Ed.* **2003**, *42*, 1743.
9. a) Kanaoka, S.; Grubbs, R. H. *Macromolecules* **1995**, *28*, 4707; b) Schwab, P.; Grubbs, R. H.; Ziller, J. W. *J. Am. Chem. Soc.* **1996**, *118*, 100; c) Weck, M.; Schwab, P.; Grubbs, R. H. *Macromolecules* **1996**, *29*, 1789.

10. Scholl, M.; Ding, S.; Lee, C. W.; Grubbs, R. H. *Org. Lett.* **1999**, *1*, 953.
11. a) Chatterjee, A. K.; Grubbs, R. H. *Org. Lett.* **1999**, *1*, 1751; b) Chatterjee, A. K.; Morgan, J. P.; Scholl, M.; Grubbs, R. H. *J. Am. Chem. Soc.* **2000**, *122*, 3783; c) Choi, T.-L.; Chatterjee, A. K.; Grubbs, R. H. *Angew. Chem.* **2001**, *113*, 1317; *Angew. Chem, Int. Ed.* **2001**, *40*, 1277; d) Chatterjee, A. K.; Choi, T.-L.; Grubbs, R. H. *Synlett.* **2001**, 1034; e) Choi, T.-L.; Lee, C. W.; Chatterjee, A. K.; Grubbs, R. H. *J. Am. Chem. Soc.* **2001**, *123*, 10417; f) Choi, T.-L.; Grubbs, R. H. *Chem. Commun.* **2001**, 2648; g) Lee, C. W.; Choi, T.-L.; Grubbs, R. H. *J. Am. Chem. Soc.* **2002**, *124*, 3224.
12. a) Sanford, M. S.; Ulman, M.; Grubbs, R. H. *J. Am. Chem. Soc.* **2001**, *123*, 749; b) Sanford, M. S.; Love, J. A.; Grubbs, R. H. *J. Am. Chem. Soc.* **2001**, *123*, 6543.
13. Choi, T.-L.; Rutenberg, I. M.; Grubbs, R. H. *Angew. Chem, Int. Ed.* **2002**, *41*, 3839.
14. ROMP with catalyst **3** gives extremely high molecular weight polymers that are often insoluble, but low PDIs have been observed, see: Maynard, H. D.; Okada, S. Y.; Grubbs, R. H. *Macromolecules*, **2000**, *33*, 6239.
15. Love, J. A.; Morgan, J. P.; Trnka, T. M.; Grubbs, R. H. *Angew. Chem, Int. Ed.* **2002**, *41*, 4035.
16. Khosravi, E.; Feast, W. J.; Al-Hajaji, A. A.; Leejarkpai, T. *J. Mol. Catal. A: Chemical* **2000**, *160*, 1.
17. Moffitt, M.; Khougas, K.; Eisenberg, A. *Acc. Chem. Res.* **1996**, *29*, 95.
18. Kataoka, K.; Harada, A.; Nagasaki, Y. *Adv. Drug Delivery Rev.* **2001**, *47*, 113.
19. a) Moffitt, M.; Vali, H.; Eisenberg, A. *Chem, Mater.* **1998**, *10*, 1021; b) Klingelhofer, S.; Heitz, W.; Greiner, A.; Oestreich, S.; Forster, S.; Antonietti, M. *J. Am. Chem. Soc.* **1997**, *119*, 10116.
20. a) Saito, R.; Kotsubo, H.; Ishizu, K. *Polymer*, **1991**, *27*, 1153; b) Guo, A.; Liu, G.; Tao, J. *Macromolecules* **1996**, *29*, 2487.
21. For a recent review, see: Wooley, K. L. *J. Polym. Sci. Part A: Polym Chem.* **2000**, *38*,

1397.

22. Butun, V.; Armes, S. P.; Billingham, N. C. *Macromolecules* **2001**, *34*, 1148.
23. a) Widawski, G.; Rawiso, M.; Francois, B. *Nature* **1994**, *369*, 387; b) Jenekhe S. A.; Chen, X. L. *Science* **1999**, *283*, 372; c) Srinivasarao, M.; Collings, D.; Philips, A.; Patel, S. *Science* **2001**, *292*, 79.